Article

Revolutionizing Solar Power Forecasts by Correcting the Outputs of the WRF-SOLAR Model

Cheng-Liang Huang [1], Yuan-Kang Wu [1,*], Chin-Cheng Tsai [2], Jing-Shan Hong [2] and Yuan-Yao Li [3,4]

[1] Department of Electrical Engineering, National Chung Cheng University, Chia-Yi 62102, Taiwan; steven810831@hotmail.com
[2] Meteorology and Information Center, Central Weather Bureau, Taipei 100006, Taiwan; cctsai@cwb.gov.tw (C.-C.T.); rfs14@cwb.gov.tw (J.-S.H.)
[3] Department of Chemical Engineering, National Chung Cheng University, Chia-Yi 62102, Taiwan; chmyyl@ccu.edu.tw
[4] Advanced Institute of Manufacturing with High-Tech Innovations, National Chung Cheng University, Chia-Yi 62102, Taiwan
[*] Correspondence: allenwu@ccu.edu.tw; Tel.: +886-5-2720411 (ext. 33232)

Abstract: Climate change poses a significant threat to humanity. Achieving net-zero emissions is a key goal in many countries. Among various energy resources, solar power generation is one of the prominent renewable energy sources. Previous studies have demonstrated that post-processing techniques such as bias correction can enhance the accuracy of solar power forecasting based on numerical weather prediction (NWP) models. To improve the post-processing technique, this study proposes a new day-ahead forecasting framework that integrates weather research and forecasting solar (WRF-Solar) irradiances and the total solar power generation measurements for five cities in northern, central, and southern Taiwan. The WRF-Solar irradiances generated by the Taiwan Central Weather Bureau (CWB) were first subjected to bias correction using the decaying average (DA) method. Then, the effectiveness of this correction method was verified, which led to an improvement of 22% in the forecasting capability from the WRF-Solar model. Subsequently, the WRF-Solar irradiances after bias correction using the DA method were utilized as inputs into the transformer model to predict the day-ahead total solar power generation. The experimental results demonstrate that the application of bias-corrected WRF-Solar irradiances enhances the accuracy of day-ahead solar power forecasts by 15% compared with experiments conducted without bias correction. These findings highlight the necessity of correcting numerical weather predictions to improve the accuracy of solar power forecasts.

Keywords: bias correction; solar irradiance prediction; decaying average; solar power forecasting

1. Introduction

Under the concept of reducing global warming and promoting zero-carbon emissions, the development of new energy sources and energy conservation has become a significant topic for many countries. Due to limited natural resources, Taiwan currently relies on imports for 97% of its energy supply. To achieve energy autonomy and diversification, the primary goal in Taiwan is to develop self-generated energy and decentralized energy sources. Taiwan is located in the subtropical zone with high solar irradiances, so it is a suitable area to develop solar power generation.

Solar power generation is highly correlated with solar irradiance, and a numerical weather prediction (NWP) model to estimate solar irradiance is significant for solar power forecasting [1]. The most advanced NWP model designed for solar energy is WRF-Solar, a mesoscale professional meteorological model based on the weather research and forecasting (WRF) model [2,3]. It is specifically designed to provide resource assessment and solar power forecasts [4–6]. Although the WRF-Solar model has made numerous improvements

and optimizations to the parameterization process of WRF irradiances, it does not consider the effect of dynamic aerosol processes on solar irradiance [7]. In other words, an incomplete understanding of the dynamical laws of weather events would hinder accurate predictions. Under a clear sky, aerosols directly affect the forecasting accuracy of global horizontal irradiance (GHI) and direct normal irradiance, making them the largest source of uncertainty [8]. Therefore, improving the forecasting accuracy of aerosol optical thickness under clear sky conditions is crucial [9,10]. While the meteorological parameters of a specific region can be investigated using specialized meteorological instruments, collecting meteorological data worldwide is currently not feasible. Therefore, data-driven and machine learning (ML) approaches for NWP bias correction have become an important trend [11].

The bias correction of deterministic predictions by WRF-Solar is a critical aspect that needs to be addressed, especially to ensure a high accuracy on GHI forecasts. Accurate GHI predictions are essential for the widespread adoption of grid-connected photovoltaic (PV) installations. For deterministic forecasting models, two commonly used post-processing methods for bias correction are model output statistics (MOS) and Kalman filtering. MOS, initially introduced by the National Weather Service in the United States, aims to reduce bias in an NWP output model through post-processing [12]. The major concept of MOS is to represent the bias in NWP forecasts with a regression function. Once a regression function is fitted, it can be used to predict the bias. To enhance the solar irradiance forecasts made by NWP models, various regression methods have been employed, such as multivariate linear regressions with stepwise variable selection [13–15], probability-based distributions [16,17], and other bias correction techniques. That is, there are numerous options for regression methods. Many data-driven or ML methods can be combined with regression functions for bias correction. One approach utilized a clear-sky model with an artificial neural network to correct the GHI in the integrated forecasting system [18]. Additionally, an optimization method based on extreme-learning machines was applied to predict the missing values in a solar irradiance dataset, achieving a high forecasting accuracy [19]. The ν-support vector regression was utilized to enhance ML-based methods for day-ahead solar irradiance prediction, and the results showed a great improvement compared with the Japan Meteorological Agency mesoscale model [20]. The ML methods described so far have followed the concept of shallow network learning models for correction and prediction. However, these shallow network models provide poor methods for feature selection, which cannot handle the high complexity of extensive datasets. Consequently, this drives more advanced and promising correction and prediction methods.

Deep learning (DL), a subfield of ML, has garnered rapid popularity in recent years owing to hardware and software advancements. Notably, the self-attention mechanism of DL enables it to automatically discern and capture long-range dependencies within a sequence during processing [21]. This empowers DL models to grasp contextual nuances and intricate patterns within a sequence, rendering it suitable for tasks in natural-language processing and sequence modeling [22]. As a result, numerous self-attention-based network models have been further developed to improve the forecasting accuracy of solar irradiance. Noteworthy examples include the robust self-attention multi-horizon model based on the transformer model [23], the spatial and temporal attention-based neural network in conjunction with federated learning techniques [24], and the Informer model [25]. However, such a self-attention mechanism has drawbacks, including its complexity, large resource demands, and computational costs, which hinder its scalability and efficiency, especially in resource-constrained environments.

In contrast to the batch post-processing approach of MOS, Kalman filtering is another sequential method for post-processing. It has been a significant engineering concept for various scientific fields, including solar energy applications [26–28]. Among the different variants of Kalman filtering, the decaying average (DA) method applies the principles of Kalman filtering and utilizes a simple mathematical approach to calculate the systematic bias correction in the model. Up to now, solar energy applications using the DA

method are few in the literature, although they have been applied in the context of surface temperature [29,30], daily maximum temperature [31], rainfall [32], and wind speed [33]. Nevertheless, they have been formally implemented in online ensemble forecasts by the National Centers for Environmental Prediction and the Meteorological Service of Canada [34]. These studies have demonstrated the success of the DA method to improve NWP forecasts, rendering them more accurate and aligned with actual forecasting operations. The DA method provides the advantage of adaptively capturing short-term variations by assigning greater weights to the recent data, rendering it suitable for real-time applications and non-stationary data. It does not need substantial historical data for calibration [35]. Due to its simplicity and reduced risk of overfitting, many works have further enhanced the computational efficiency of the DA method and achieved rapid adaptation to data trends [36]. Some research works have explored its potential applications in the field of renewable energy [37–39]. Although the DA method has been employed to correct weather forecasts, it still has a largely unexplored potential to forecast solar power generation.

To resolve the above-mentioned research gaps, this paper proposes a comprehensive solar power forecasting procedure that integrates NWP correction. The novelty of this study lies in the development of a DA method based on the Kalman filter; additionally, this method refines daily raw solar irradiance forecasts obtained by the WRF-Solar forecasting model developed by the Taiwan Central Weather Bureau (CWB). To validate the efficiency of the post-processing method, WRF-Solar irradiance forecasts at five cities spanning different latitudes and longitudes were collected with the aim to verify the applicability of the DA method across diverse geographical regions. Additionally, this study compared the performance between the DA method and the transformer model for WRF-Solar bias correction. In collaboration with PV sites in five cities, the PV power generation data from local PV sites were also aggregated. The bias-corrected WRF-Solar irradiances were then combined with the total solar power generation to obtain day-ahead total solar power deterministic forecasts. The operational viability of this forecasting framework has been successfully demonstrated in this paper. The content of this paper includes the following main items:

1. The Pearson correlation analysis was used to select representative meteorological sites in five cities. These cities are located in northern, central, and southern Taiwan.
2. An analysis of the discrepancy between the WRF-Solar irradiances and the observed solar irradiances was carried out at the selected meteorological sites in each city.
3. The development of a post-processing algorithm using the DA method was proposed. It considers WRF-Solar irradiance forecasts as inputs to generate day-ahead bias-corrected WRF-Solar irradiance forecasts at five cities. This study implemented the validation and comparison for the outputs of the WRF-Solar model using the DA method, the original WRF-Solar forecast model, or the transformer model. In addition, this study utilized diverse performance evaluation metrics, including mean error (ME) and root-mean-square error (RMSE).
4. The WRF-Solar model, after undergoing post-processing with the DA method, was combined with the total solar power generation at each city to predict solar power generation. It aims to generate day-ahead total power generation forecasts. Subsequently, these forecasting results were validated and compared against the results using the original WRF-Solar forecast model and the transformer model with several performance evaluation metrics, including RMSE, normalized RMSE (nRMSE), mean absolute error (MAE), mean absolute percentage error (MAPE), and R-squared (R^2).

The paper is divided into four sections: Section 1 is the introduction; Section 2 describes the WRF-Solar prediction model and the two post-processing algorithms; Section 3 presents the forecasting results and analyses; Section 4 discusses the results of the review; and Section 5 draws the conclusions.

2. Methods

The framework of this study is presented in Figure 1 and is divided into three main parts. In the first part, the WRF-Solar meteorological sites at the five cities were selected using Pearson correlation analysis. That is, representative WRF-Solar meteorological sites were subsequently selected at each city based on their correlations with the total solar power generation. Figure 2 displays the number of WRF-Solar meteorological sites and solar power sites at each of the five cities. From northern to southern Taiwan, there are four WRF-Solar meteorological sites in Taoyuan, ten sites in Taichung, seven sites in Tainan, five sites in Kaohsiung, and nine sites in Pingtung. As for PV power stations, Taoyuan, Taichung, Tainan, Kaohsiung, and Pingtung include 30, 14, 18, 21, and 14 sites, respectively. The historical data recorded from the WRF-Solar meteorological sites and PV power stations cover the period from January to December 2019. The second part of Figure 1 shows that the representative WRF-Solar irradiances at each city were further corrected for bias using the DA method. The corrected performance was subsequently compared with that of the transformer model. The third part of Figure 1 shows that the bias-corrected WRF-Solar irradiances obtained through the DA method were combined with the total solar power generation for PV power forecasts. The transformer model was then employed to generate day-ahead deterministic forecasts. Additionally, the corrected performance was compared against the day-ahead deterministic forecasts generated by the transformer model using bias-corrected WRF-Solar irradiances.
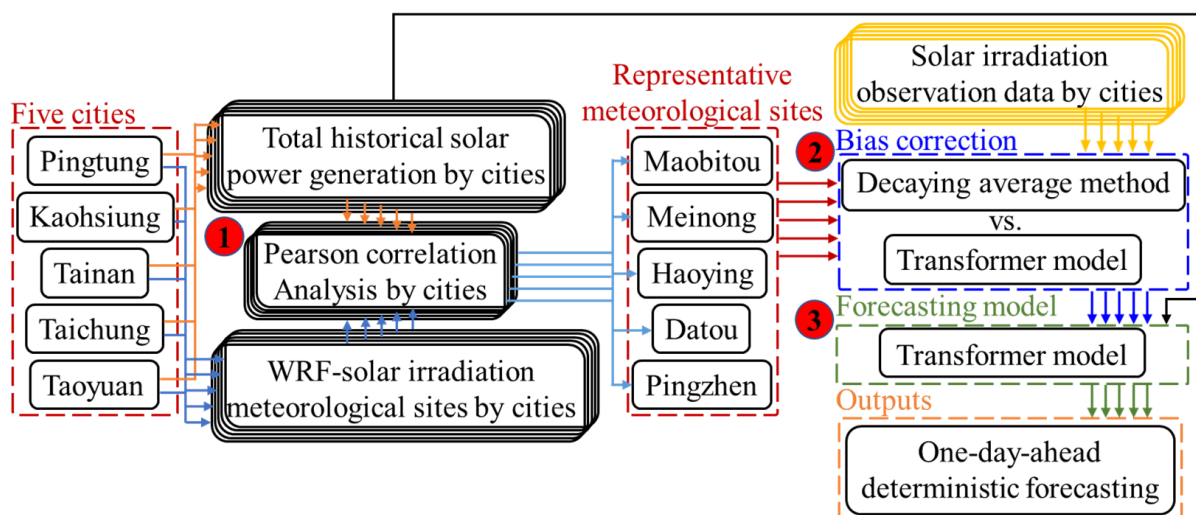

Figure 1. Scheme of the WRF-Solar irradiance bias correction and one-day-ahead solar power generation forecasting model.

In the second part, the bias-correction method for wind speeds described in our previous study [33] was used for bias correction for the WRF-Solar irradiances. The previous study employed the DA method to enhance the WRF ensemble wind speed forecasts in Taiwan. However, in this study, the weighting coefficients were predefined in the DA method for the solar power application (these weighting coefficients are introduced in Section 2.2) and set the training window for WRF-Solar irradiances at approximately two months. This approach aims to emphasize the weighting of error samples around the analyzed time. Consequently, in this study, a fixed weighting coefficient of 0.06 was designed for the DA method, which corresponds to a two-month training period. To evaluate the adaptability of using the DA method across various geographical regions and seasons, WRF-Solar irradiances at five cities were collected and validated in spring (May), summer (August), and winter (December) to evaluate the performance after the bias-correction technique. The transformer model was used to compare the bias-correction

performance with the DA method. Therefore, the training period for the transformer model was set to two months, the same as the DA method.
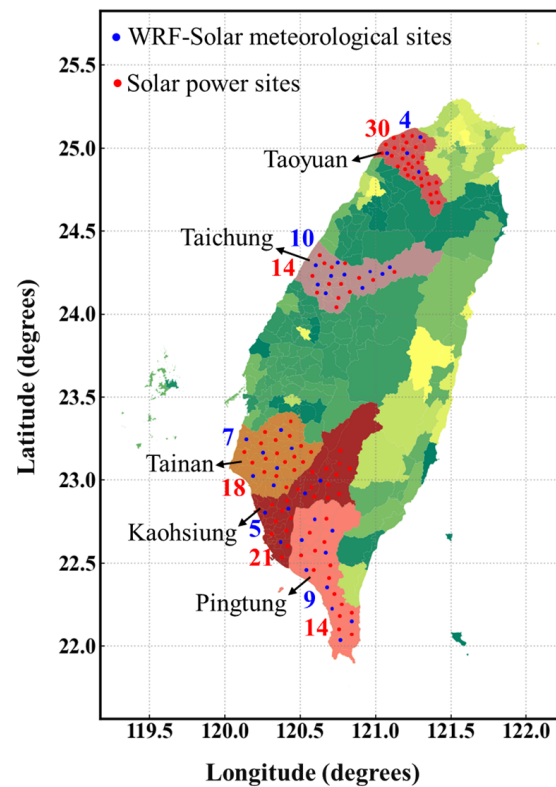

Figure 2. Number of WRF-Solar meteorological sites and solar power sites at five cities in Taiwan.

In the third part, the training model obtained in the second part with a two-month period was utilized to predict the total solar power generation. The bias-corrected WRF-Solar irradiances obtained using the DA method or the transformer model were then used as inputs into the transformer model to predict day-ahead solar power generation. This process aims to generate a day-ahead forecast for total solar power generation. Likewise, the transformer model was employed to forecast day-ahead total solar power generation by utilizing the bias-corrected WRF-Solar irradiances obtained from the transformer model itself. The following section introduces the theory of WRF-Solar, the DA method, and the transformer model.

2.1. Numerical Weather Prediction Modeling Systems–WRF-Solar

In this study, the bias correction of WRF-Solar irradiances and solar power generation forecasts was performed using the WRF-Solar model developed by Taiwan CWB. The WRF-Solar model is specialized to provide solar irradiances for various applications. The WRF-Solar model is based on version 4.3 of the community WRF model [2,3] with one-way nested domains. The horizontal grid spacing of the coarse and nested domains is equal to 15 and 3 km, respectively (Figure 3), and the vertical levels of the atmosphere are in 52 layers. The WRF-Solar model employs standardized modules that are designed specifically for solar energy applications [4–6]. Physical parameterization of the WRF-Solar model includes the Kain–Fritsch cumulus parameterization with a new trigger function [40], the Goddard 5-class scheme for microphysical parameterization [41], the Yonsei University scheme for boundary layer parameterization [42], the RRTMG scheme for long/short-wave irradiation parameterization [43], the Monin–Obukhov scheme for surface parameterization, and the NOAH soil model with four soil layers [44]. Additionally, dynamical parameters are configured using a Eulerian mass dynamical core, Runge–Kutta third order for time integration, evaluation of a second-order diffusion term on coordinate surfaces for turbulence and

mixing, and horizontal Smagorinsky first-order closure. Finally, the model of the configured WRF-Solar generates solar irradiance forecasts initialized at 0000/0600/1200/1800 Coordinated Universal Time (UTC) for each day, with each forecast providing a 120 h prediction at hourly intervals.
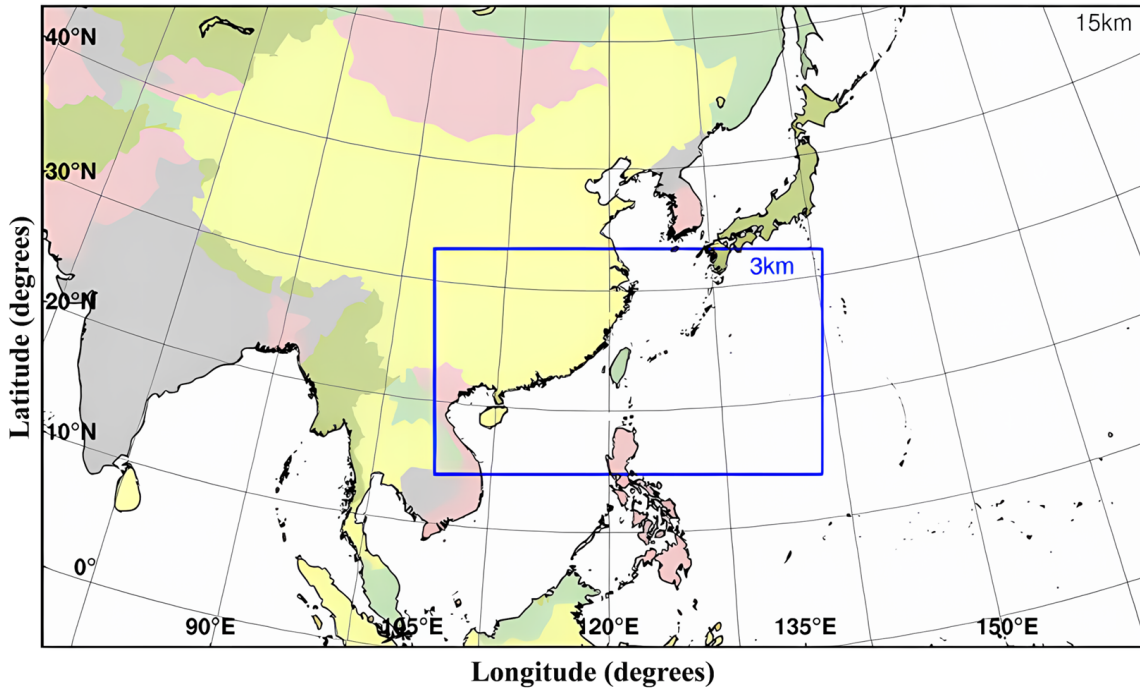

Figure 3. The covered range of WRF-Solar.

For the collection of day-ahead WRF-Solar irradiances, the 1200 UTC updated solar irradiance data from the WRF-Solar model were selected for concatenation, as shown in Figure 4. Because the initialization of running a WRF-Solar model requires a 6 h preparation time, the initial 6 h of WRF-Solar irradiances were deleted. Furthermore, because the time format of the WRF-Solar model used is based on UTC, the time zone needed to be converted to the Taiwan time zone (UTC + 8). Consequently, the starting time of the collected WRF-Solar irradiances was set at 2:00 a.m. for each day.
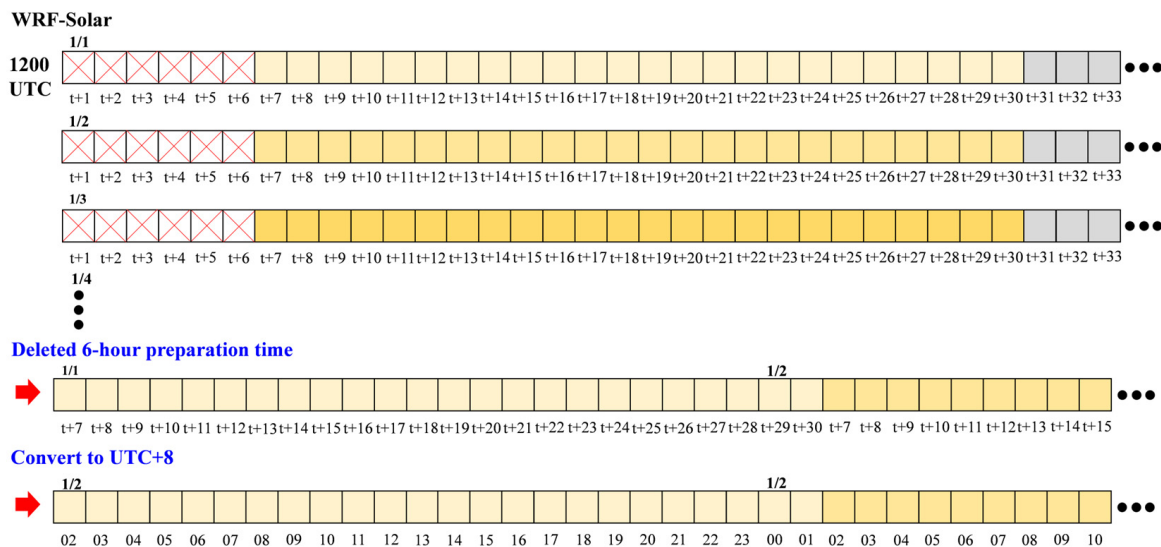

Figure 4. The schematic diagram of the concatenated WRF-Solar data.

2.2. DA Bias Correction

The DA method employs an adaptive algorithm, which is a straightforward mathematical method for the bias correction of WRF-Solar irradiances. This method uses both WRF-Solar irradiances and actual observed solar irradiances to establish the training model. The application of the DA algorithm involves three main steps: estimation of forecasting errors, estimation of systematic bias, and bias correction [29,33,34].

Step 1. Calculate the model prediction error (b_t) by the difference between the WRF-Solar irradiances (f_t) and the corresponding observed solar irradiances (o) at the same time horizon.

$$b_t = f_t - o \tag{1}$$

Step 2. Compute the systematic bias (B_t) utilizing a weight coefficient (w) including the cumulative systematic bias (b_{t-1}) and prediction error (b_{t-1}).

$$B_t = (1 - w) \times B_{t-1} + w \times b_{t-1} \tag{2}$$

Step 3. Obtain the bias-corrected WRF-Solar irradiances (F_t), which are derived based on the difference between the WRF-Solar irradiances and the systematic bias.

$$F_t = f_t - B_t \tag{3}$$

2.3. Transformer Model

The transformer model is an architecture with neural networks initially developed for natural language translation that has gained widespread applications in various domains [22]. Unlike recursive or convolutional models, the transformer model utilizes an attention mechanism to capture global information [21]. The model consists of two essential components, the encoder and the decoder, as shown in Figure 5. The encoder aims to encode the input sequence. It consists of multiple stacked encoder layers, which are structurally identical but do not share parameters between layers. Each encoder layer contains two sub-layers: a fully connected feedforward layer and a multi-head attention (MHA) layer. The encoder aims to extract key spatial information from WRF-Solar irradiances. Subsequently, this key spatial information is input into the decoder. The decoder decodes the output sequence from the encoder. Similar to the encoder, it consists of a stack of *N* identical decoder layers. The distinction between encoder and decoder is that the decoder includes a masked MHA layer preceding the MHA layer. The masking prevents the predicted input from influencing subsequent positions. In this study, the SoftMax layer that originally appeared in the decoder was removed because this study focused on deterministic predictions instead of probabilistic predictions [45]. The decoder combines the potential spatial WRF-Solar irradiances from the encoder to predict day-ahead WRF-Solar irradiance. Furthermore, in this study, the WRF-Solar irradiances corrected by the DA method or the transformer model were utilized for solar power generation forecasting via a transformer model. The input of the transformer model encoder was changed from the uncorrected WRF-Solar irradiances to the corrected WRF-Solar irradiances. Moreover, the corrected WRF-Solar irradiances were further encoded and were used as the input of the decoder. Finally, the decoder was used to forecast the total power generation using the corrected WRF-Solar irradiances. In this study, the transformer model consists of two layers at both encoder and decoder with a dimension of 64 (typical default value) in the input layer and a multi-head attention (the head number is two). The computer employed in this study was equipped with an Intel Core i9-9900K processor (Intel, Santa Clara, CA, USA), an NVIDIA RTX 2080Ti GPU (NVIDIA, Santa Clara, CA, USA), and 64GB of RAM. The transformer model was executed using Python software (Python 3.6) with Keras (version 2.10.0), TensorFlow(version 2.6.2), and Sklearn libraries (version

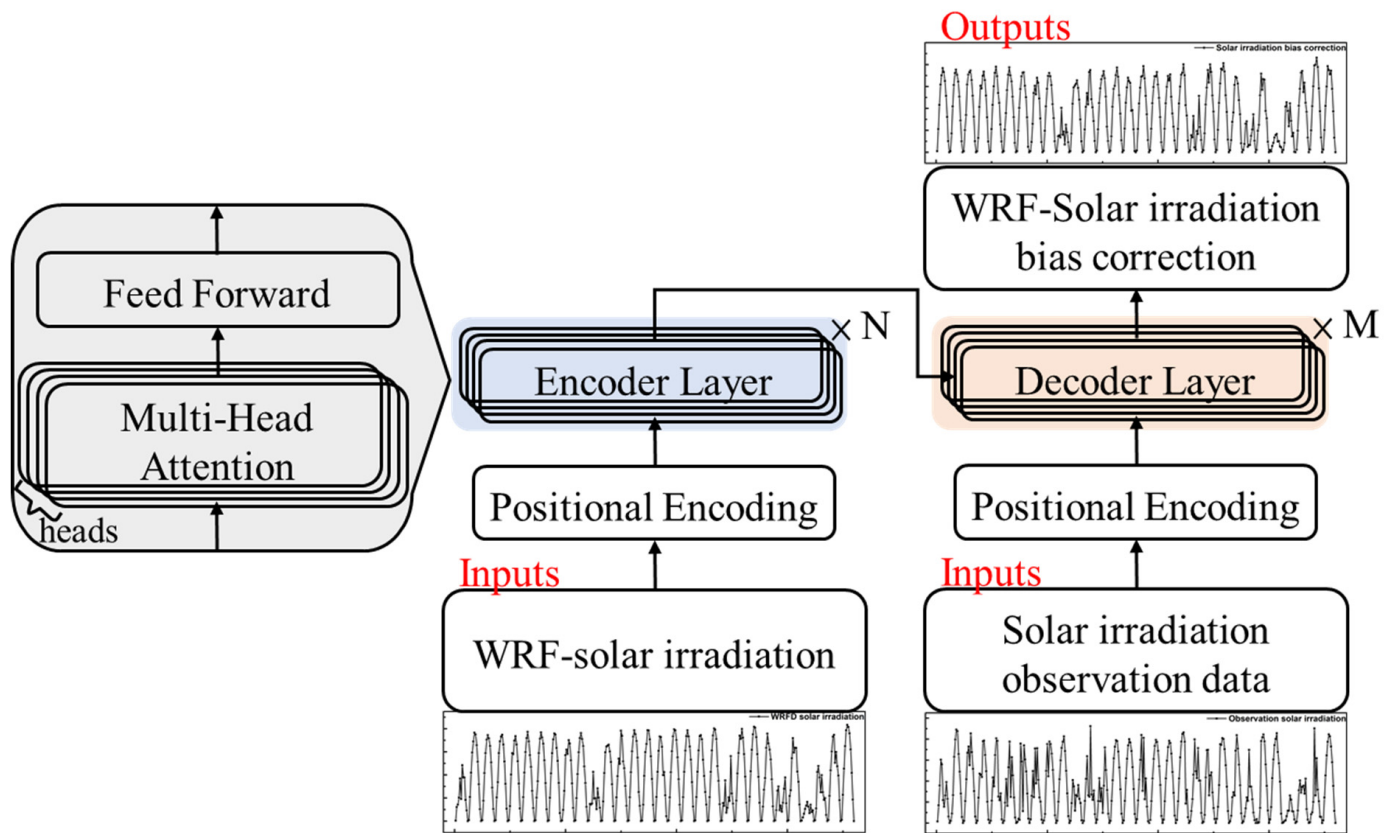0.24.2), where identical hyperparameters were applied across all experiments to maintain a fair result.

Figure 5. Architecture of transformer forecasting model for WRF-Solar irradiance bias correction.

3. Results

3.1. Pearson Correlation Analysis

The representative meteorological sites at each city were selected based on their highest correlation with the total solar power generation using Pearson correlation analysis. The following representative meteorological sites at the five cities were identified: Maobitou meteorological site for Pingtung county, Meinong meteorological site for Kaohsiung county, Haoying meteorological site for Tainan county, Datou meteorological site for Taichung county, and Pingzhen meteorological site for Taoyuan county. The correlation coefficients between the observed solar irradiances and the total PV power generation at each city were 0.8539, 0.8823, 0.9019, 0.86, and 0.872, respectively, as illustrated in Figure 6a–e. Moreover, in this study, the WRF-Solar irradiances at the five cities were further bias-corrected.
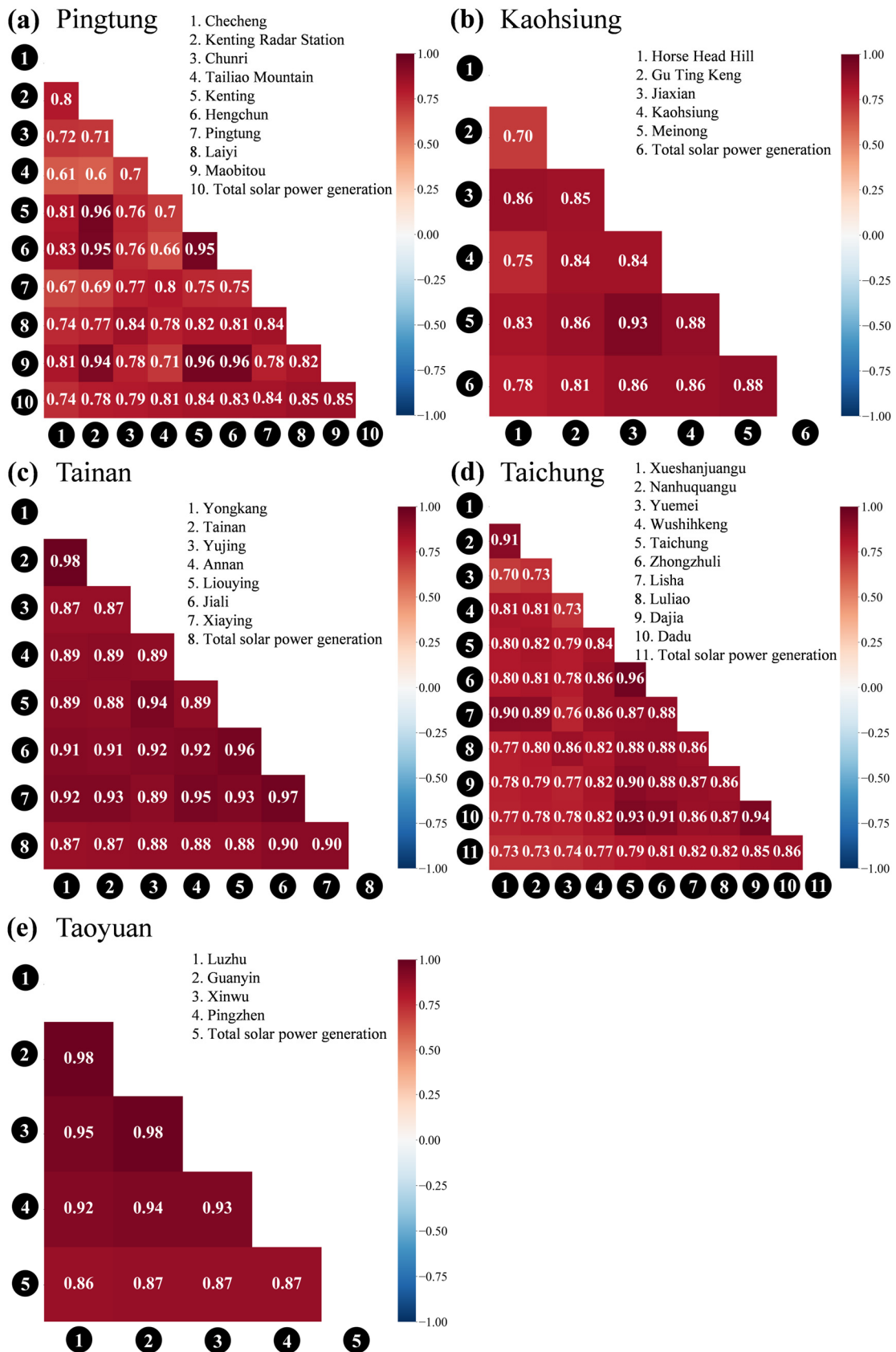
Figure 6. Pearson correlation analysis of WRF-Solar meteorological sites and total solar power generation in (**a**) Pingtung, (**b**) Kaohsiung, (**c**) Tainan, (**d**) Taichung, and (**e**) Taoyuan cities in Taiwan.

3.2. Bias Correction for WRF-Solar Irradiances

It is important to understand the ME and probability density function (PDF) bias level of the representative WRF-Solar irradiances and the observed solar irradiances at the five cities, as shown in Figure 7a–j. The results indicate that the WRF-Solar irradiances in Taoyuan in December are comparable to the observed solar irradiances, with an average ME of 3.46 W/m^2. Additionally, the PDF shows an overestimation for low solar irradiances and an underestimation for high solar irradiances, as shown in Figure 7i,j. Moreover, both the ME (Figure 7a,c,e,g,i) and PDF (Figure 7b,d,f,h,j) clearly demonstrate that the generated WRF-Solar irradiances at the cities of Pingtung, Kaohsiung, Tainan, and Taichung were consistently overestimated in May, August, and December. This indicates that WRF-Solar irradiances must be corrected for the forecasting biases.

In this study, the DA method was employed for the bias correction of the WRF-Solar irradiances, and the performance of its correction is presented in Table 1, which demonstrates that at the five cities, using the DA method achieved an improvement in the WRF-Solar irradiances during the three validation months. The RMSE index is reduced from the uncorrected solar irradiance of 137.91 W/m^2 to the corrected solar irradiance of 107.94 W/m^2, which causes a reduction in error of 22%. Except for Taoyuan in December, using the DA method did not result in an improvement. As shown in Table 1, after the bias correction with the DA method, the forecasting accuracy of solar irradiance is reduced by 2.5%. This discrepancy could be attributed to the nature of the DA method, which accumulates systematic errors over the past two months to correct for bias on the validation date. In cases when the correction bias in the validation month is smaller but the correction bias in the preceding two months is larger, it could cause an inability to correct the validation data. However, for most areas and seasons, bias correction using the DA method does improve the accuracy of solar irradiances from the WRF-Solar.

Table 1. The RMSE and error reduction rate of the WRF-Solar irradiance after bias correction using methods 1, 2, and 3 in five cities.

City	Months	Before Bias Correction RMSE (W/m^2)	After Bias Correction			
			DA Method		Transformer Model	
			RMSE (W/m^2)	Reduced (%)	RMSE (W/m^2)	Reduced (%)
Pingtung	May	182.09	172.06	5.51	162.16	10.94
	August	243.77	237.41	2.61	227.65	6.61
	December	143.97	130.83	9.13	112.40	21.93
Kaohsiung	May	227.48	213.58	6.11	212.91	6.41
	August	227.45	217.70	4.29	195.51	14.04
	December	143.28	122.14	14.75	96.91	32.36
Tainan	May	210.56	201.78	4.17	190.21	9.67
	August	204.14	202.98	0.57	202.29	0.91
	December	127.47	117.71	7.66	94.86	25.58
Taichung	May	222.96	181.48	18.60	168.39	24.48
	August	212.20	195.48	7.88	179.06	15.62
	December	137.91	107.94	21.73	102.68	25.55
Taoyuan	May	257.42	205.40	20.21	174.32	32.28
	August	247.47	223.16	9.82	191.24	22.72
	December	158.39	162.37	−2.51	128.32	18.98

To further investigate the reason for the low accuracy in a particular month in Taoyuan, this study analyzed the differences between the WRF-Solar irradiances and observed solar irradiances. Figure 8 shows the bias levels between the WRF-Solar irradiances and observed solar irradiances, as measured with ME (Figure 8a) and PDF (Figure 8b), in October and November in Taoyuan. It shows that the WRF-Solar irradiances at 2:00 p.m. and 3:00 p.m.

in October and November are overestimated, with an average ME of 29.81 W/m^2 and 22.80 W/m^2 in October and November, respectively, which causes a low accuracy using the DA method. These observations emphasize the limitations of using the DA method.
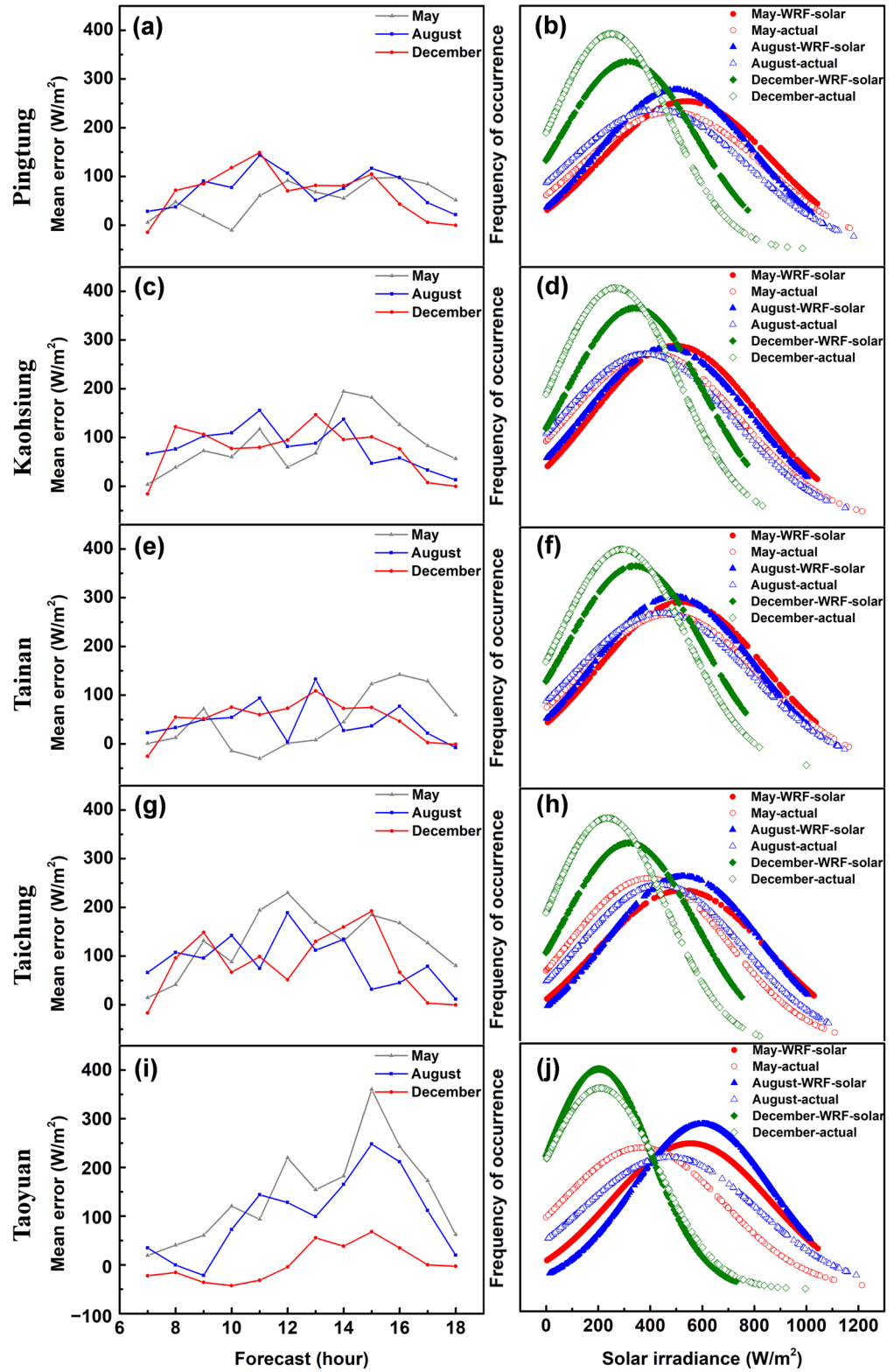

Figure 7. (**a**,**c**,**e**,**g**,**i**) Mean error and (**b**,**d**,**f**,**h**,**j**) probability density function of WRF-Solar irradiance before bias correction in five cities.

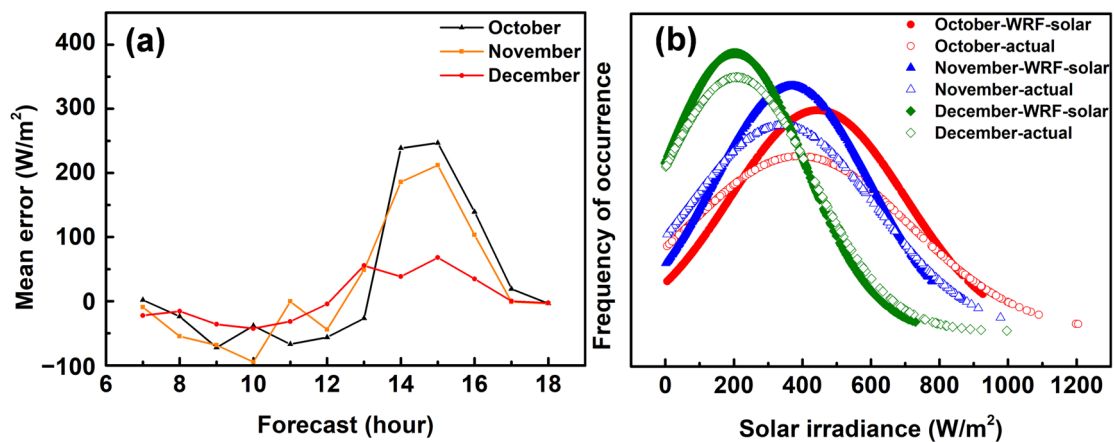**Figure 8.** (**a**) Mean error and (**b**) probability density function of WRF-Solar irradiance before bias correction in Taoyuan.

In northern Taiwan, the winter season typically begins around December, leading to a large influence of the northeast monsoon. As a result, the temperature gradually drops with the strengthening of the northeast winds. In winter, the average solar irradiance is reduced. To enhance the effectiveness of the DA bias correction method, future work will focus on resolving the observed systematic bias at meteorological sites in northern Taiwan. Therefore, the update on the outputs of the WRF-Solar model will be increased or the accumulated time of the systematic biases will be reduced. Those strategies aim to mitigate the impact of previously accumulated systematic biases on the following forecasts. Furthermore, it is expected that the DA method will be improved by incorporating additional meteorological variables, such as wind direction, wind speed, temperature, and humidity, into the training model. In addition, the use of AI algorithms is expected to obtain a comprehensive relationship between surface solar irradiances and three-dimensional meteorological variables. Thus, these AI algorithms could provide another appropriate solution to improve the outputs of the WRF-Solar model.

To make a comparison with the DA method, the bias correction of the WRF-Solar irradiances was also performed using a transformer model. As shown in Table 1, the transformer model used mostly outperforms the DA method for the performance of bias correction. However, at some cities, the DA method outperformed the transformer model in specific months, such as Kaohsiung in May and Tainan in August. Additionally, in terms of calculation speed, the DA method operated in 4.4 s, while the transformer model needs 119.4 s. Thus, the runtime cost clearly highlights the advantages of the DA method, aligning with its simplicity and enhanced computational efficiency [36].

3.3. Solar Power Generation Forecasting

The WRF-Solar irradiances at the five cities, with or without bias correction with the DA method, were input into the transformer model to predict day-ahead solar power generation in the validation months. Tables 2 and 3 illustrate that the accuracy of the total solar power generation forecasts for the three validation months at the five cities can be effectively improved by 15.5% when the DA method is applied for bias correction. The exception case appears in Taoyuan, where the accuracy of power generation forecasting in December is worse than that using uncorrected WRF-Solar irradiances, as indicated in Table 3. This phenomenon was caused owing to the limitation of the bias correction of WRF-Solar irradiances, as previously discussed in Section 3.2. That is, the limitation of the bias correction would affect the accuracy of solar power forecasts. It also reaffirms the strong positive correlation between the accuracy of WRF-Solar irradiance and PV power forecasting.

To make a comparison with the solar power forecasts using the DA method, bias-corrected WRF-Solar irradiances obtained via the transformer model were also employed to

make one-day-ahead forecasts of total solar power generation. The results in Tables 2 and 3 show an improvement in the accuracy of the WRF-Solar irradiances using the transformer model. However, even though the WRF-Solar irradiances corrected with the transformer model are closer to the observed solar irradiances, there is no substantial enhancement in the total power generation forecasting, because the total power generation was forecasted based on the observed solar irradiances from the representative meteorological sites rather than the sites of specific power plants. The solar power plants are located in diverse geographical areas within the city, while the climatic conditions would be different at the representative meteorological sites. As a result, there will be estimation errors for solar irradiances.

Table 2. The one-day-ahead forecast results of total solar power generation in Pingtung, Kaohsiung, Tainan, and Taichung using WRF-Solar irradiance with and without bias correction.

City	Months	Methods	RMSE (W)	nRMSE (%)	MAE (W)	MAPE (%)	R^2 (%)
Pingtung	May	Before bias correction	2118.87	13.29	1287.14	8.07	79.44
		DA method	1957.19	12.28	1207.37	7.57	82.45
		Transformer model	1849.35	11.60	1185.52	7.44	84.33
	August	Before bias correction	2227.58	14.65	1692.58	11.13	72.17
		DA method	2154.01	14.17	1623.41	11.02	73.98
		Transformer model	2118.61	13.93	1611.56	10.68	74.82
	December	Before bias correction	1698.62	13.90	1223.60	10.02	75.28
		DA method	1604.67	13.14	1178.58	9.65	77.94
		Transformer model	1555.35	12.73	1091.10	8.93	79.27
Kaohsiung	May	Before bias correction	4226.87	14.23	2946.49	9.92	78.37
		DA method	4100.81	13.81	2725.49	9.18	79.64
		Transformer model	3830.50	12.90	2652.42	8.93	82.23
	August	Before bias correction	4469.14	15.28	3347.43	11.45	72.23
		DA method	4438.45	15.18	2991.87	10.23	72.61
		Transformer model	4036.69	13.80	2721.62	9.31	77.34
	December	Before bias correction	2677.56	11.32	1735.40	7.34	84.86
		DA method	2261.43	9.56	1480.10	6.26	89.20
		Transformer model	2082.34	8.80	1454.93	6.15	90.85
Tainan	May	Before bias correction	4193.26	12.42	2715.35	8.04	81.06
		DA method	4042.27	11.97	2625.39	7.77	82.40
		Transformer model	3338.59	9.89	2477.87	7.34	88.00
	August	Before bias correction	4640.92	15.08	3131.87	10.18	73.59
		DA method	4414.95	14.34	3064.75	9.96	76.10
		Transformer model	3859.47	12.54	2805.88	9.12	81.74
	December	Before bias correction	2966.53	11.28	2212.21	8.41	84.21
		DA method	2962.36	11.26	2084.70	7.92	84.25
		Transformer model	2470.29	9.39	1665.25	6.33	89.05
Taichung	May	Before bias correction	5571.37	15.22	3566.67	9.74	71.32
		DA method	5328.13	14.55	3628.38	9.91	73.77
		Transformer model	4353.12	11.89	3001.43	8.20	82.49
	August	Before bias correction	5857.03	16.21	4538.94	12.57	63.46
		DA method	5782.84	16.01	4537.32	12.56	64.38
		Transformer model	5563.80	15.40	4233.96	11.72	67.03
	December	Before bias correction	3984.67	12.66	2772.05	8.81	81.20
		DA method	3652.22	11.60	2643.75	8.40	84.21
		Transformer model	3577.11	11.36	2633.85	8.37	84.84

Table 3. The one-day-ahead forecast results of total solar power generation in Taoyuan using WRF-Solar irradiance with and without bias correction.

City	Months	Methods	RMSE (W)	nRMSE (%)	MAE (W)	MAPE (%)	R^2 (%)
Taoyuan	May	Before bias correction	7528.52	15.40	4662.42	9.54	70.84
		DA method	6924.99	14.17	4643.39	9.50	75.33
		Transformer model	5463.58	11.18	3697.08	7.56	84.64
	August	Before bias correction	4941.93	10.33	3531.97	7.38	86.22
		DA method	4849.74	10.14	3423.61	7.16	86.73
		Transformer model	4243.30	8.87	3346.17	7.00	89.84
	December	Before bias correction	4478.30	11.72	3078.46	8.06	68.44
		DA method	5320.82	13.93	3833.73	10.04	55.45
		Transformer model	4365.33	11.43	2934.81	7.68	70.01

In summary, the use of the WRF-Solar model is effective to estimate total power generation when WRF-Solar irradiances are bias-corrected successfully using the DA method. This highlights the necessity of the bias correction technique for WRF-Solar and reaffirms the viability of the DA method. The primary contribution of this study is to apply the DA method to bias-correct WRF-Solar irradiances and then use the result of the WRF-Solar corrections for solar power generation forecasting. It improves on the disadvantages of the previous literature, which focused only on the bias correction of meteorological factors without further considering renewable power forecasting.

4. Discussion

This study employed the DA method to correct and refine the output of the WRF-Solar model and utilized the bias correction of solar irradiances to input the forecasting model for the day-ahead forecasting of solar power generation. The DA method has demonstrated its effectiveness in correcting other meteorological parameters such as temperature, wind speed, etc. [29–33]. However, it is noteworthy that the performance of this method was not validated for solar irradiance before. Nevertheless, this paper successfully demonstrates the application of the DA method on the bias correction of the solar irradiances from the WRF-Solar model, which identifies several gaps in our current knowledge.

Furthermore, the reliability of solar power generation forecasts is attributed to the WRF-Solar model produced by Taiwan CWB. The model provides valuable solar irradiances with the highest horizontal resolution of 3 km and a lead time of 120 h for deterministic forecasts, and the predicted solar irradiances are updated four times daily. Then, the output from the WRF-Solar model serves as input for the day-ahead forecasting of solar power generation. This paper explores how the WRF-Solar model can be used to provide useful and valuable weather forecasts for solar power forecasts in Taiwan.

Regarding the limitations of the DA method, the main constraint comes from its statistical nature, because the DA method relies on historical data. As a result, it may exhibit limitations in accurately predicting extreme weather events that could occur in the future. This is a significant limitation of using the DA method. To deal with short-term extreme weather events, such as a rapid change in solar irradiances or wind speeds, it is recommended to use a new NWP model to replace the DA method. This NWP model can combine its outputs with real-time observations to update the forecast quickly. In other words, the new NWP model can update the output rapidly and generate a short-term weather forecast for the next 12 h. Furthermore, utilizing AI-related algorithms can also provide post-processing products and apply to various weather forecasts. These AI algorithms can train the forecasting model through a long-term three-dimensional meteorological dataset and combine NWP forecasts with real-time observations to improve forecasting accuracy.

5. Conclusions

In this study, a comprehensive framework for day-ahead solar power generation forecasts has been proposed. The primary contribution of this paper is to introduce a novel application using the DA method to correct WRF-Solar irradiances across five distinct geographic locations and different seasons. Moreover, the corrected WRF-Solar irradiances were combined with total solar power generation to generate deterministic day-ahead total solar power forecasting. The aforementioned procedures were compared with a transformer model to assess the effectiveness of using the DA method for WRF-Solar irradiance correction and solar power forecasts. The developed framework has been validated across five cities in Taiwan, covering diverse geographic regions (north, central, and south) and seasonal variations (spring, summer, and winter), yielding outstanding results.

The results after bias correction demonstrate that the DA method effectively corrects the WRF-Solar irradiances, improving the accuracy of WRF-Solar irradiances (with a 22% reduction in error) and reducing computational time from 119.4 s to 4.4 s. Notably, although the DA method provided acceptable bias corrections in most cases, it could not fully correct the bias due to its systematic bias accumulation, which presents a limit to using this method. Nevertheless, the advantage of its simplicity should not be underestimated. The results of day-ahead solar power generation forecasts show that the bias correction of WRF-Solar irradiances through the DA method enhances the forecasting accuracy by 15.5%. In conclusion, this study highlights the significance of bias correction in WRF-Solar irradiances to improve solar power generation forecasts.

Author Contributions: Conceptualization, C.-L.H. and Y.-K.W.; methodology, C.-L.H. and Y.-K.W.; software, C.-L.H.; validation, Y.-K.W. and Y.-Y.L.; formal analysis, C.-L.H.; investigation, C.-L.H.; resources, C.-L.H., Y.-K.W., C.-C.T. and J.-S.H.; writing—original draft preparation, C.-L.H., Y.-K.W., and Y.-Y.L.; writing—review and editing, Y.-K.W.; supervision, Y.-K.W. and Y.-Y.L.; project administration, Y.-K.W. All authors have read and agreed to the published version of the manuscript.

Data Availability Statement: Data are contained within the article.

Conflicts of Interest: The authors declare no conflict of interest.

Nomenclature

NWP	Numerical weather prediction
WRF-Solar	Weather research and forecasting solar
WRF	Weather research and forecasting
CWB	Central Weather Bureau
DA	Decaying average
GHI	Global horizontal irradiance
PV	Photovoltaic
MOS	Model output statistics
ML	Machine learning
DL	Deep learning
ME	Mean error
RMSE	Root-mean-square error
nRMSE	Normalized root-mean-square error
MAE	Mean absolute error
MAPE	Mean absolute percentage error
R^2	R-squared
UTC	Coordinated Universal Time
MHA	Multi-head attention
PDF	Probability density function

References

1. Ahmed, R.; Sreeram, V.; Mishra, Y.; Arif, M. A review and evaluation of the state-of-the-art in PV solar power forecasting: Techniques and optimization. *Renew. Sustain. Energy Rev.* **2020**, *124*, 109792. [CrossRef]
2. Skamarock, W.C.; Klemp, J.B.; Dudhia, J.; Gill, D.O.; Liu, Z.; Berner, J.; Wang, W.; Powers, J.; Duda, M.; Barker, D. *A Description of the Advanced Research WRF Version 4*; National Center for Atmospheric Research (NCAR): Boulder, CO, USA, 2019; Volume 145.
3. Powers, J.G.; Klemp, J.B.; Skamarock, W.C.; Davis, C.A.; Dudhia, J.; Gill, D.O.; Coen, J.L.; Gochis, D.J.; Ahmadov, R.; Peckham, S.E. The weather research and forecasting model: Overview, system efforts, and future directions. *Bull. Am. Meteorol. Soc.* **2017**, *98*, 1717–1737. [CrossRef]
4. Jimenez, P.A.; Hacker, J.P.; Dudhia, J.; Haupt, S.E.; Ruiz-Arias, J.A.; Gueymard, C.A.; Thompson, G.; Eidhammer, T.; Deng, A. WRF-Solar: Description and clear-sky assessment of an augmented NWP model for solar power prediction. *Bull. Am. Meteorol. Soc.* **2016**, *97*, 1249–1264. [CrossRef]
5. Jiménez, P.A.; Alessandrini, S.; Haupt, S.E.; Deng, A.; Kosovic, B.; Lee, J.A.; Delle Monache, L. The role of unresolved clouds on short-range global horizontal irradiance predictability. *Mon. Weather Rev.* **2016**, *144*, 3099–3107. [CrossRef]
6. Haupt, S.E.; Kosovic, B.; Jensen, T.; Lee, J.; Jimenez, P.; Lazo, J.; Cowie, J.; McCandless, T.; Pearson, J.; Weiner, G. *The SunCast Solar-Power Forecasting System: The Results of the Public-Private-Academic Partnership to Advance Solar Power Forecasting*; National Center for Atmospheric Research (NCAR): Boulder, CO, USA, 2016.
7. Liu, Y.; Qian, Y.; Feng, S.; Berg, L.K.; Juliano, T.W.; Jiménez, P.A.; Liu, Y. Sensitivity of solar irradiance to model parameters in cloud and aerosol treatments of WRF-solar. *Sol. Energy* **2022**, *233*, 446–460. [CrossRef]
8. Gueymard, C.A. Temporal variability in direct and global irradiance at various time scales as affected by aerosols. *Sol. Energy* **2012**, *86*, 3544–3553. [CrossRef]
9. Randles, C.A.; Kinne, S.; Myhre, G.; Schulz, M.; Stier, P.; Fischer, J.; Doppler, L.; Highwood, E.; Ryder, C.; Harris, B. Intercomparison of shortwave radiative transfer schemes in global aerosol modeling: Results from the AeroCom Radiative Transfer Experiment. *Atmos. Chem. Phys.* **2013**, *13*, 2347–2379. [CrossRef]
10. Ruiz-Arias, J.A.; Dudhia, J.; Santos-Alamillos, F.J.; Pozo-Vázquez, D. Surface clear-sky shortwave radiative closure intercomparisons in the Weather Research and Forecasting model. *J. Geophys. Res. Atmos.* **2013**, *118*, 9901–9913. [CrossRef]
11. Yang, D.; van der Meer, D. Post-processing in solar forecasting: Ten overarching thinking tools. *Renew. Sustain. Energy Rev.* **2021**, *140*, 110735. [CrossRef]
12. Glahn, H.R.; Lowry, D.A. The use of model output statistics (MOS) in objective weather forecasting. *J. Appl. Meteorol. Climatol.* **1972**, *11*, 1203–1211. [CrossRef]
13. Verzijlbergh, R.A.; Heijnen, P.W.; de Roode, S.R.; Los, A.; Jonker, H.J. Improved model output statistics of numerical weather prediction based irradiance forecasts for solar power applications. *Sol. Energy* **2015**, *118*, 634–645. [CrossRef]
14. Lopes, F.M.; Conceição, R.; Silva, H.G.; Salgado, R.; Collares-Pereira, M. Improved ECMWF forecasts of direct normal irradiance: A tool for better operational strategies in concentrating solar power plants. *Renew. Energy* **2021**, *163*, 755–771. [CrossRef]
15. Verbois, H.; Huva, R.; Rusydi, A.; Walsh, W. Solar irradiance forecasting in the tropics using numerical weather prediction and statistical learning. *Sol. Energy* **2018**, *162*, 265–277. [CrossRef]
16. Li, T.; Hui, P.; Tang, J.; Fang, J. Future projections of wind and solar energy resources over China from regional climate models based on bias correction. *Environ. Res. Commun.* **2023**, *5*, 061004. [CrossRef]
17. Dieng, D.; Cannon, A.J.; Laux, P.; Hald, C.; Adeyeri, O.; Rahimi, J.; Srivastava, A.K.; Mbaye, M.L.; Kunstmann, H. Multivariate bias-correction of high-resolution regional climate change simulations for West Africa: Performance and climate change implications. *J. Geophys. Res. Atmos.* **2022**, *127*, e2021JD034836. [CrossRef]
18. Pereira, S.; Canhoto, P.; Salgado, R.; Costa, M.J. Development of an ANN based corrective algorithm of the operational ECMWF global horizontal irradiation forecasts. *Sol. Energy* **2019**, *185*, 387–405. [CrossRef]
19. Boriratrit, S.; Fuangfoo, P.; Srithapon, C.; Chatthaworn, R. Adaptive meta-learning extreme learning machine with golden eagle optimization and logistic map for forecasting the incomplete data of solar irradiance. *Energy AI* **2023**, *13*, 100243. [CrossRef]
20. Gari da Silva Fonseca Jr., J.; Uno, F.; Ohtake, H.; Oozeki, T.; Ogimoto, K. Enhancements in day-ahead forecasts of solar irradiation with machine learning: A novel analysis with the Japanese mesoscale model. *J. Appl. Meteorol. Climatol.* **2020**, *59*, 1011–1028. [CrossRef]
21. Bahdanau, D.; Cho, K.; Bengio, Y. Neural machine translation by jointly learning to align and translate. *arXiv* **2014**, arXiv:1409.0473.
22. Vaswani, A.; Shazeer, N.; Parmar, N.; Uszkoreit, J.; Jones, L.; Gomez, A.N.; Kaiser, Ł.; Polosukhin, I. Attention is all you need. *Adv. Neural Inf. Process. Syst.* **2017**, *30*, 5998–6008.
23. Sharda, S.; Singh, M.; Sharma, K. RSAM: Robust self-attention based multi-horizon model for solar irradiance forecasting. *IEEE Trans. Sustain. Energy* **2020**, *12*, 1394–1405. [CrossRef]
24. Wen, H.; Du, Y.; Lim, E.G.; Wen, H.; Yan, K.; Li, X.; Jiang, L. A solar forecasting framework based on federated learning and distributed computing. *Build. Environ.* **2022**, *225*, 109556. [CrossRef]
25. Jiang, C.; Zhu, Q. Evaluating the most significant input parameters for forecasting global solar radiation of different sequences based on Informer. *Appl. Energy* **2023**, *348*, 121544. [CrossRef]
26. Pelland, S.; Galanis, G.; Kallos, G. Solar and photovoltaic forecasting through post-processing of the Global Environmental Multiscale numerical weather prediction model. *Prog. Photovolt. Res. Appl.* **2013**, *21*, 284–296. [CrossRef]

27. Liu, Y. Solar GHI Ensemble Prediction Based on a Meteorological Model and Method Kalman Filter. *Adv. Meteorol.* **2022**, *2022*, 1523198. [CrossRef]

28. Yang, D. On post-processing day-ahead NWP forecasts using Kalman filtering. *Sol. Energy* **2019**, *182*, 179–181. [CrossRef]

29. Chen, Y.; Hong, J. Bias Correction of Surface Temperature Prediction by Using the Decaying Average Algorithm. *Atmos. Sci. (Meteorol. Soc. ROC)* **2017**, *45*, 25–42.

30. Boyd, P.; Phillips, W. Predicting Surface Temperatures of Roads: Utilizing a Decaying Average in Forecasting. *J. Purdue Undergrad. Res.* **2016**, *6*, 3. [CrossRef]

31. Belorid, M.; Kim, K.R.; Cho, C. Bias Correction of short-range ensemble forecasts of daily maximum temperature using decaying average. *Asia-Pac. J. Atmos. Sci.* **2020**, *56*, 503–514. [CrossRef]

32. Kaewmesri, P. Improving Rainfall Performance by Decaying Average Bias Correction via Lyapunov Theory. *GEOMATE J.* **2020**, *19*, 49–56. [CrossRef]

33. Tsai, C.-C.; Hong, J.-S.; Chang, P.-L.; Chen, Y.-R.; Su, Y.-J.; Li, C.-H. Application of bias correction to improve WRF ensemble wind speed forecast. *Atmosphere* **2021**, *12*, 1688. [CrossRef]

34. Cui, B.; Toth, Z.; Zhu, Y.; Hou, D. Bias correction for global ensemble forecast. *Weather Forecast.* **2012**, *27*, 396–410. [CrossRef]

35. Singh, H.; Dube, A.; Kumar, S.; Ashrit, R. Bias correction of maximum temperature forecasts over India during March–May 2017. *J. Earth Syst. Sci.* **2020**, *129*, 1–10. [CrossRef]

36. Guan, H.; Cui, B.; Zhu, Y. Improvement of statistical postprocessing using GEFS reforecast information. *Weather Forecast.* **2015**, *30*, 841–854. [CrossRef]

37. Hamill, T.M. Comparing and combining deterministic surface temperature postprocessing methods over the United States. *Mon. Weather Rev.* **2021**, *149*, 3289–3298. [CrossRef]

38. Gong, L.; Peng, Z.; Wei, Z.; Zhang, B.; Dong, J.; Chen, H.; Cai, J.; Zhang, Q.; Zhang, F. Medium-to long-term forecast of reference crop evapotranspiration based on the correction of the principal control factor. *Irrig. Drain.* **2022**, *71*, 912–925. [CrossRef]

39. Zhao, L.; Lu, S.; Qi, D. Improvement of Maximum Air Temperature Forecasts Using a Stacking Ensemble Technique. *Atmosphere* **2023**, *14*, 600. [CrossRef]

40. Kain, J.S. The Kain–Fritsch convective parameterization: An update. *J. Appl. Meteorol.* **2004**, *43*, 170–181. [CrossRef]

41. Tao, W.-K.; Simpson, J.; Baker, D.; Braun, S.; Chou, M.-D.; Ferrier, B.; Johnson, D.; Khain, A.; Lang, S.; Lynn, B. Microphysics, radiation and surface processes in the Goddard Cumulus Ensemble (GCE) model. *Meteorol. Atmos. Phys.* **2003**, *82*, 97–137. [CrossRef]

42. Hong, S.-Y.; Noh, Y.; Dudhia, J. A new vertical diffusion package with an explicit treatment of entrainment processes. *Mon. Weather Rev.* **2006**, *134*, 2318–2341. [CrossRef]

43. Iacono, M.J.; Delamere, J.S.; Mlawer, E.J.; Shephard, M.W.; Clough, S.A.; Collins, W.D. Radiative forcing by long-lived greenhouse gases: Calculations with the AER radiative transfer models. *J. Geophys. Res. Atmos.* **2008**, *113*, D13103. [CrossRef]

44. Mukul Tewari, N.; Tewari, M.; Chen, F.; Wang, W.; Dudhia, J.; LeMone, M.; Mitchell, K.; Ek, M.; Gayno, G.; Wegiel, J. Implementation and Verification of the Unified NOAH land Surface Model in the WRF Model (Formerly Paper Number 17.5). In Proceedings of the 20th Conference on Weather Analysis and Forecasting/16th Conference on Numerical Weather Prediction, Seattle, WA, USA, 14 January 2004.

45. Qu, K.; Si, G.; Shan, Z.; Kong, X.; Yang, X. Short-term forecasting for multiple wind farms based on transformer model. *Energy Rep.* **2022**, *8*, 483–490. [CrossRef]